Validation of spectral finite element simulation tools dedicated to guided wave based structure health monitoring

Cite as: AIP Conference Proceedings **2102**, 050018 (2019); https://doi.org/10.1063/1.5099784
Published Online: 08 May 2019

Olivier Mesnil, Alexandre Imperiale, Edouard Demaldent, and Bastien Chapuis

Validation of Spectral Finite Element Simulation Tools Dedicated to Guided Wave Based Structure Health Monitoring

Olivier Mesnil[1,a)], Alexandre Imperiale[1], Edouard Demaldent[1], Bastien Chapuis[1]

[1] *NDE department CEA LIST, Saclay, France*

[a)]Corresponding author: Olivier.mesnil@cea.fr

Abstract. Guided Wave based SHM (GW-SHM) relies on the use of elastic guided waves to interrogate plates or unidirectional structures such as pipes for defects and has received considerable attention from the literature in the past few years. Despite a large number of in-lab setups and more mature prototypes, GW-SHM finds no high-maturity applications outside the pipeline industry. Indeed, the complexity of the GW propagation phenomena inhibits the demonstration of reliability of GW-SHM. In other words, in order to ensure the efficiency of GW-SHM system on real-life situations with varying environmental conditions and exploitation constraints, a huge number of experiments are to be conducted. In order to quantify the robustness and efficiency of the GW-SHM systems, dedicated simulations tools have been developed and released in the CIVA software. These tools rely on spectral finite elements and a dedicated meshing strategy to ensure fast but reliable computation. Compared to current commercial finite elements tools, computation times are reduced by 2 to 3 orders of magnitude. This communication presents the validation of such tools in GW-SHM configuration. Simulated signals are compared to experimental ones for both isotropic and anisotropic panels. Results of guided wave imaging algorithms are compared between simulated and experimental datasets.

INTRODUCTION

Structural Health Monitoring (SHM) consists of permanently installing sensors onto or into a structure in order to continuously or periodically monitor its health in a non-destructive fashion. The main objective of SHM is to certify the health of the structure until the next maintenance operation. SHM will eventually lead to a change of paradigm from scheduled maintenance operations towards SHM-triggered maintenance. Because sensors are permanently installed at the beginning of the structure's life, they can be placed at specific locations, for example hard to access locations for traditional Non Destructive Techniques (NDT). Finally, the structure can be continuously or periodically monitored, leading to a wealth of information regarding the structure damage behavior and eventually to a reduction of design security coefficients through a deeper understanding of the damage mechanisms.

Guided Waves (GWs) are elastic waves guided by the structure in which they propagate and are a relevant mean of interrogation to detect defects in plate-like structures. Among other things, GWs are extremely sensitive to a wide variety of defects and propagate over long distances, thus limiting the number of sensors required to monitor large areas. However, GWs are multi-modal, dispersive and sensitive to Environmental and Operating Conditions (EOC), making them complex to analyze. GW-based SHM (GW-SHM) has received significant interest from the scientific community and a very large number of in-lab GW-SHM prototypes have been documented. A common application of GW-SHM is through Guided Wave Imaging (GWI) aiming at creating images representing the health of the inspected structures [1], [2], [3], [4]. Most often, but not necessarily, GWI relies on an array of piezoelectric transducers (PZT), each acting sequentially as emitter and receiver of GWs in order to measure the propagated wave packets between every pair of sensors. In this configuration, it is assumed that the presence of a defect will somehow modify the propagation of the waves, for example with the existence of a reflected wave packet.

If such GW-SHM systems find limited applications in the pipeline industry it is not the case in the aerospace industry in which, to the authors' knowledge, no GW-SHM system is on the path to certification. Among the reasons for this lack of adoption of the technology is the need to demonstrate and quantify the performances of a GW-SHM system. Unlike in NDT where one sample of limited size with multiple defects can be used multiple times with various inspection parameters to compute a Probability of Detection (POD) curve [5], it is not possible in SHM due to the

45th Annual Review of Progress in Quantitative Nondestructive Evaluation, Volume 38
AIP Conf. Proc. 2102, 050018-1–050018-8; https://doi.org/10.1063/1.5099784
Published by AIP Publishing. 978-0-7354-1832-5/$30.00

requirement to permanently install the sensors. In other words, to demonstrate the performances of an SHM system experimentally, for every combination of parameters (typically hundreds or thousands) a representative sample would have to be manufactured, instrumented and damaged to evaluate the performance of the system, leading to a prohibitive cost.

A more credible approach is to demonstrate the performances through simulation. In practice, for every set of possible EOC and defect, a simulation must be conducted to judge the efficiency of the monitoring system. In other words, to demonstrate the performance of a given SHM system applied to a specific use-case, thousands of simulations must be computed. Currently, various Finite Element (FE) based codes allow the simulation of GW in composite materials. However, due to the characteristic temporal dimension (excitation frequencies of a few kHz to a few hundreds of kHz) and spatial dimension (wavelengths of a few millimeters to centimeters), the simulation of GW requires small time steps and spatial discretization, leading to computationally intensive simulations. A benchmark [6] published in 2018 compared multiple commercial FE codes on a specific GWs propagation problem in a composite panel. Computational times between 20 to 90 hours for a single GWs propagation are achieved, which is far from being fast enough to run a large number of cases.

In order to achieve smaller computational times, a novel numerical tool have been developed at CEA-LIST and integrated in the NDT software CIVA [7] and from now on will be referred as CIVA SHM. In the present paper, a description of the numerical scheme used to achieve fast computational times will be described. Its efficiency will be compared to other FE codes in the context of the aforementioned benchmark. As validation is essential to trust the results provided by the software, preliminary validation will be presented in a metallic case through the comparison of raw signals measured by PZT transducers and GWI results.

TRANSIENT SPECTRAL FINITE ELEMENTS TOOL FOR GW-SHM

This section describes the FE code implemented in CIVA SHM and illustrates its application in a specific use-case.

Description

In order to achieve competitive computational performances, two approaches are combined to construct the so-call transient spectral FE tool built in the CIVA SHM software. First, the Spectral Finite Element Method [8] (SFEM) is used and allows, by using high order elements, a significant reduction of the number of degrees of freedom compared to a more classical formulation. Typically, elements of order 3 to 5 are used. Second, the description of the geometry and subsequently the mesh is parameterized. The parameterization reduces significantly the quantity of information to store and allows for an optimization of the storage and access to the information. For example, the elements are stored as groups according to a coloring algorithm to ensure that no adjacent elements are stored on the same memory unit, avoiding potential data races when performing element-by-element FE operations in parallel. In practice, the studied geometry is discretized in two steps, first a macro-mesh step in which the geometry is divided in large elements. Each macro-element is treated individually and the communication between the various macro-element is ensured by the mortar element method [9]. The goal of this step is to implicitly define, through the geometry of each macro-element, relevant physical information such as the local anisotropy directions. Each unique element is then subdivided in spectral finite elements.

If the parametrization of the geometry unavoidably induces a loss of genericity in terms of geometries that can be handle by the software, it also induces huge advantages in terms of computational times. Layered structures with geometrical features such as curvature or stiffeners along with a wide variety of flaws (hole, crack, delamination, thickness loss) can be handled by the software. For more details on the formulation, the reader is invited to refer to the companion paper [10].

Benchmark

The benchmark published in [6] by Leckey et al. in Jan. 2018 was used to validate the FE formulation on a specific composite use case with a delamination and compare the computational performances. The main characteristics of the benchmark are summarized here and for more details the reader is invited to refer to the corresponding publication [6].

The studied configuration is an 8-layer composite panel of 380 x 380 x 0.92mm made of IM7/8552 Carbon Fiber Reinforced Polymer (CFRP) of layup $[0_2,90_2]_s$. A square delamination of 20 x 20mm between the second and the third layer is located 64 mm away from a piezoelectric transducer acting in thickness mode excitation and located on the opposite side of the sample. This configuration was studied in the benchmark with Abaqus, Comsol, Ansys and an in-house EFIT formulation and compared to experimental data in which the delamination was a Teflon square insert. The area of interest in the simulation is 60 x 120 mm and the guided wave propagation is simulated for a total duration of 60µs. The excitation signal is a 300 kHz 3-cycle tone burst. Perfectly Matched Layer (PML) were used in the Abaqus, Ansys and Comsol simulations in order to reduce the dimensions of the sample. However PML were not used in the simulations made with CIVA SHM. Out-of-plane velocity is extracted from each simulation over the delaminated region and its surroundings with a spacing of 0.25mm.

As a first step, the macro-mesh is generated around the parameterized geometry leading to the macro mesh of Figure 1a. The macro-mesh is automatically generated around the notable features of the configuration: the square delamination, the circular transducer (both in red) and the edges of the sample. As expected, the macro elements are relatively big (a few centimeters each) and discretize the region of interest in similar regions. The micro-mesh is represented in Figure 1b. For comparison purposes, this picture is analogous to the Figure 2 of [6].

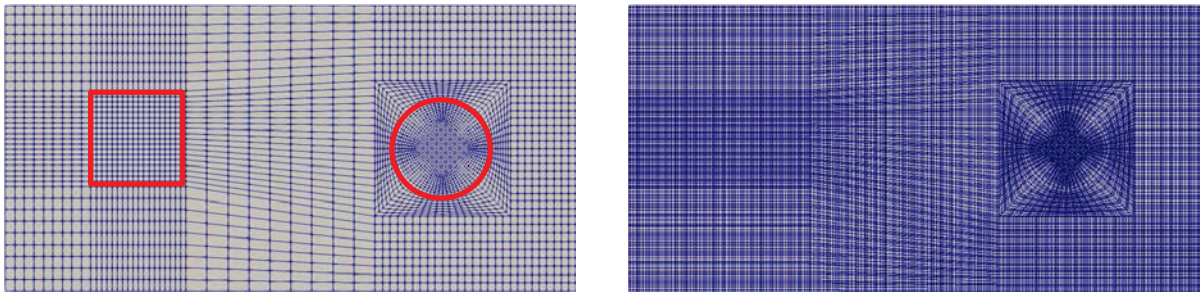

(a) (b)

Figure 1: Example of mesh obtained for the benchmark by CIVA SHM (a): macro-mesh with the delamination (red square) and transducer (red circle) and (b): spectral finite element mesh

The simulation is then conducted with the aforementioned parameters and snapshot of the guided wave propagation are extracted over the delaminated area and are represented in Figure 2a and Figure 2b at 30 µs and 40 µs after the excitation respectively. In these representations, only the out-of-plane velocity is represented meaning that only the A0 mode is visible since the S0 mode is mostly in-plane. Mode conversion from the S0 mode into the A0 mode due to the interaction of the S0 with the delamination can however be observed in Figure 2a. At the second time step, the guided wave propagation is visually slowed down over the delaminated area. These figures are to be compared with Figures 6 and 7 from [6] and a very good visual agreement is observed.

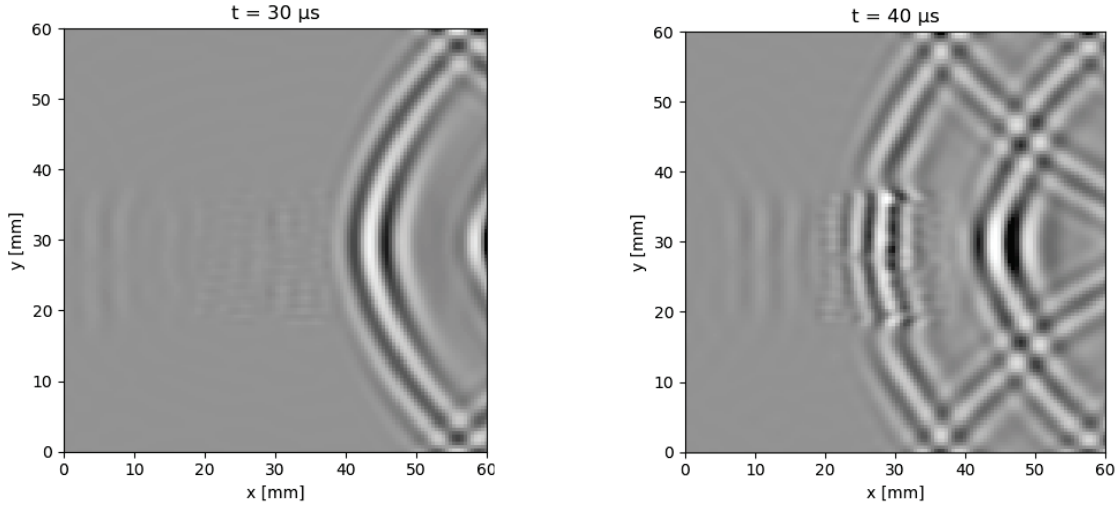

(a) (b)

Figure 2: Snapshot of the out-of-plane wave velocity over the delaminated area (a): at 30µs and (b): and 40µs

Wavenumber quantitative values at the central excitation frequency are then compared for each solver in the **Table 1**, reproduced, at the exception of the last line, from [6]. The pristine wavenumber, in both the horizontal (k_x) and the vertical (k_y) directions matches very well between CIVA SHM and the various FE solver, as well as the experiment conducted in the benchmark. The wavenumber over the delaminated region lands within the range of values provided by the benchmark even though on the upper side of it. This is most likely due to the lack of refinement of the mesh over the delaminated region in CIVA SHM, which will be added in a subsequent study.

Method	**k_x (1/m) – pristine**	**k_y (1/m) – pristine**	**k_x (1/m) – delamination**
Experiment	200.2	253.9	273.4
DISPERSE	229.5	269.5	294.1
EFIT/E	220.8	254.8	305.7
COMSOL/I	225.0	275.0	348.9
ABAQUS/I	225.0	262.5	250.4
ABAQUS/E	220.0	255.0	250.0
ANSYS/I	225.0	243.7	290.0
CIVA SHM	**220.4**	**256.3**	**320.0**

Table 1: Wavenumber obtained by the various methods at the central frequency. Table reproduced from [6] with the exception of the last line, added for comparison.

Similarly, the computational performances of each FE software are compared in **Table 2**, reproduced from [6] except for the last line. The computation with CIVA SHM is of the order of 12 minutes for this specific case while it goes from 19.5 hours to 170 hours for the various software studied by the benchmark, leading to an improvement between two to three orders of magnitude in terms of computation time. As a side note, the hardware used in the simulation with CIVA SHM is also far less efficient than the ones used in the benchmark, so a greater computational performance gap might be expected if the test was achieved on the same computer. Finally, the memory footprint of the simulation is of the order of 130MB with CIVA SHM which is negligible for current computers. This small memory footprint means that a large number of computations can be run in parallel with no risk of memory saturation.

Method	**Computational time (hours)**	**Number of cores**	**Memory (GB)**
EFIT	91	72	142
COMSOL	19.5	16	266
ABAQUS/I	40	16	28
ABAQUS/E	53	16	30
ANSYS	170	16	16
CIVA SHM	**0.2 (~12 minutes)**	**8**	**16 (actual memory footprint : 0.13GB)**

Table 2: Computational performances obtained by the various methods. Table reproduced from [6] with the exception of the last line, added for comparison.

VALIDATION

Before being able to trust the software for performance demonstration, a significant validation campaign must be conducted. This section present a preliminary validation campaign.

Raw signal comparison

The studied configuration is represented in Figure 3 and is a 400 x 400 x 3 mm aluminum plate instrumented by a circle of eight circular piezoelectric transducers. In order to study reproducibility of the GW signals using the symmetry of the system, the circle of transducer is centered on the plate and its diameter is 200 mm so that multiple guided wave path are supposedly identical. Eight identical paths are represented by the blue arrows in the Figure 3.The guided wave propagation is measured in a round-robin fashion: each transducer is sequentially actuated while measuring with the other seven. A 10mm hole is then drilled 20mm away from the center of the plate and the same measurement process is repeated.

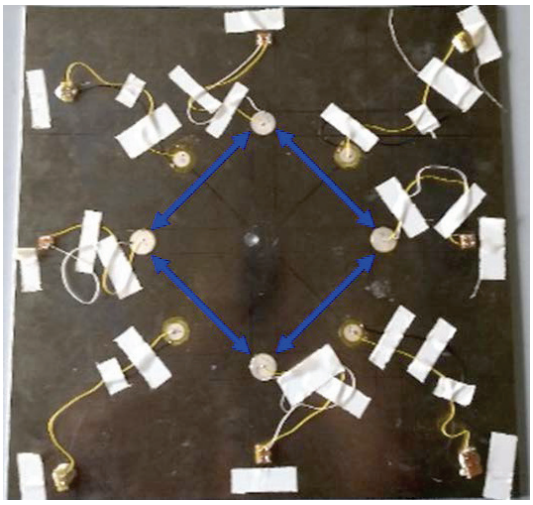

Figure 3: Picture of the studied plate: a square aluminum plate instrumented by 8 sensors. The blue arrows represent the eight guided wave paths shown in blue in **Figure 4**

The same configuration is simulated through CIVA SHM. The raw signal results for both the simulation and the experiment are superimposed in Figure 4. In blue in this figure, the experimental signals corresponding to eight previously mentioned paths are represented. Note that the eight blue signals are nearly identical with each other but do present some difference between each other due to the error during the positioning of the transducer and potentially the variability between every transducer and their bounding conditions. In red are represented the eight simulated signals corresponding to the same paths. As expected the red curves perfectly overlap with each other due to the symmetry of the configuration so only one is visible.

The overall overlap between the experimental and simulated curves is now be discussed. First, from approximately t = 0 to t = 0.025ms, an harmonic is visible in the experimental signal but not the simulated one. These oscillations are not due to a physical wavepacket but to the electronic coupling within the acquisitions devices replicating a scaled-down excitation signal. It is therefore not a physical signal that must be reproduced in the simulation. Next from t = 0.03ms to 0.06 ms the first wavepacket, the S0 mode, is measured, followed by the A0 mode from t = 0.06 ms to 0.09 ms. For both these wavepackets the agreement between the simulation and the experiment is very good but not perfect due to the variability between the experimental paths. The overlap can however be judged as “good enough” because the variability between the experimental curves and the simulated curves is of the same order of magnitude as the variability between the experimental curves themselves. In other words, the simulation is able to accurately simulate the signal within the experimental variability.

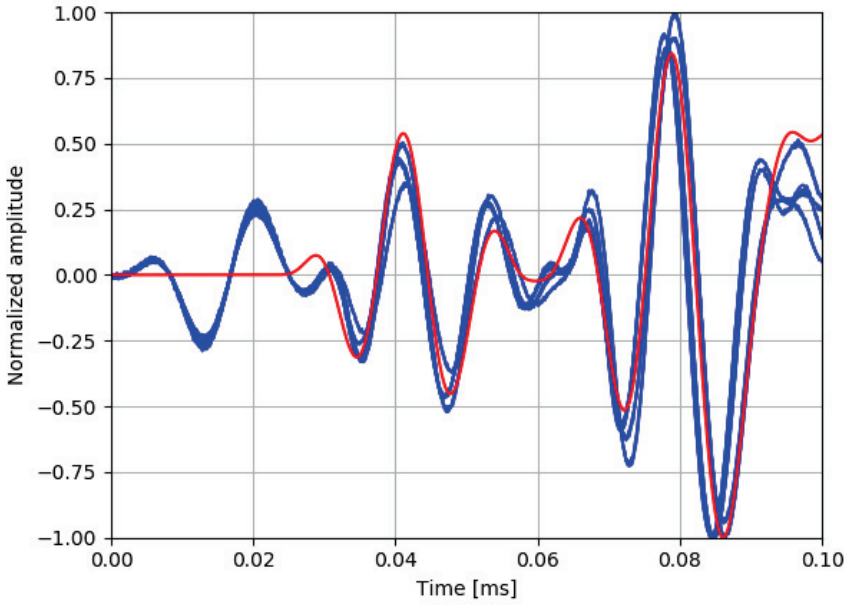

Figure 4: Comparison of the raw signals in red (simulated with CIVA SHM) and blue measured experimentally for the paths symmetrically identical

Guided wave imaging

Guided Wave Imaging (GWI) consist of creating a cartography of the structure's health. In most cases, GWI requires three components: the round robin scan of the pristine plate, the round robin scan of the plate in a potentially damaged state, and some information about the wave propagation in the structure, for example the propagation speed. Three GWI algorithms are applied to the aluminum panel in order to map the hole in the plate, namely the RAPID [1], the Delay and Sum (DAS) [2] and the Minimum Variance (MV) [3] methodologies. The approaches will not be described here but details can be found in the corresponding references.

The result of the GWI process is found in Figure 5 in which the top line shows the results for the experimental data sets for RAPID, DAS and MV processes respectively and the bottom line for the simulated dataset in the same order. It is immediately noted that the 6 pictures successfully detect and locate the defect, meaning that a yellow spot stands out from the background color, indicating the presence of some sort of flaw reflecting the waves. The performances of each algorithm are unequal due to assumptions made to interpret the data, but this is not the topic of this paper. The agreement between the experimental and simulated picture is however excellent in all three cases, meaning that CIVA SHM successfully simulates the whole configuration. As expected, the experimental (top) pictures are slightly noisier that the simulated ones in which no artificial noise was added.

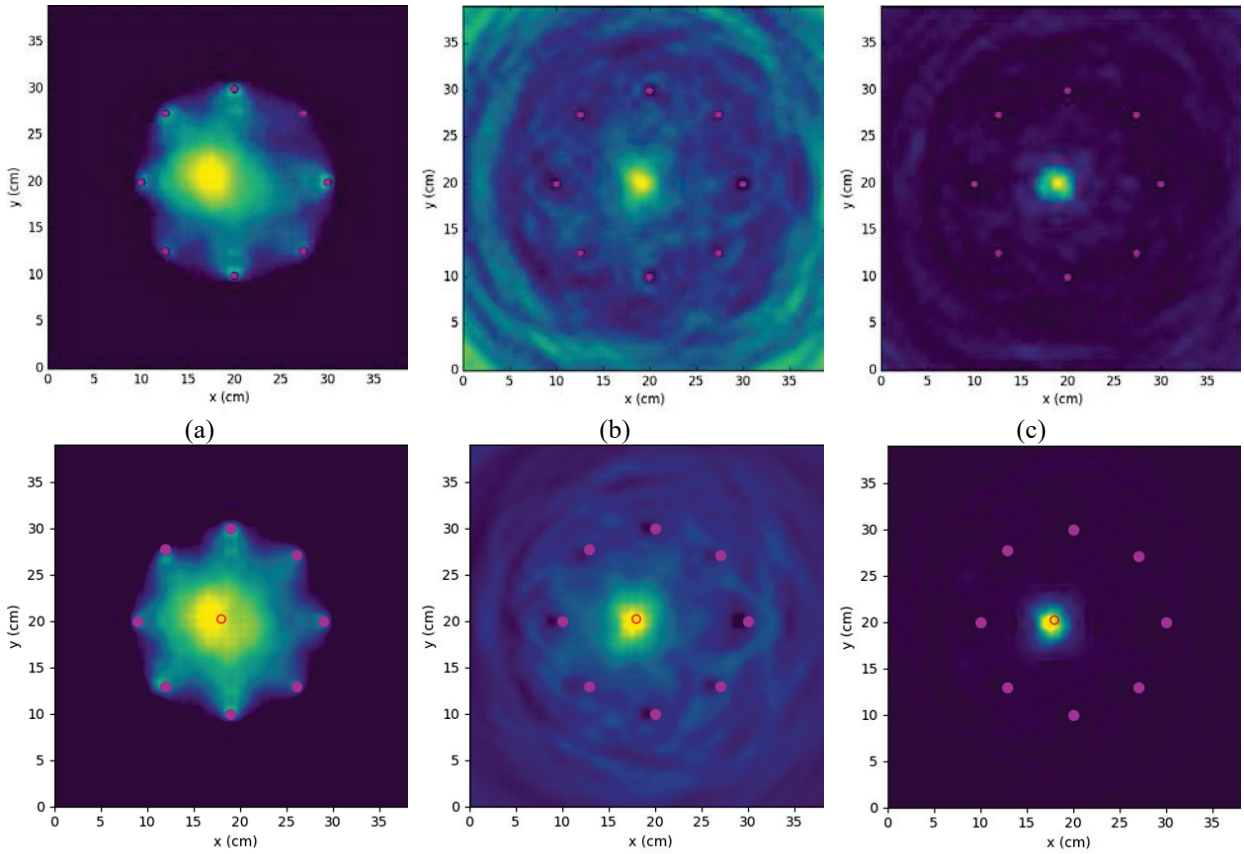

Figure 5: Comparison of guided wave imaging results obtained experimentally (top) and numerically (bottom) with the algorithms RAPID (a and d), Delay and Sum (b and e) and Minimum Variance (c and f).

CONCLUSION

The article introduces the transient spectral finite element code implemented in CIVA SHM along with a first validation step. The FE code was compared to commercial finite element software through a recent benchmark and found to be at least 100 faster on the specific use case. The code was then validated against experimental data on an isotropic panel through raw guided wave signal comparison and guided wave imaging. The results of the validation is satisfactory, but a much more extensive validation campaign must be undertaken to fully validate the software.

The combination of both faster computational times and small memory footprint is the necessary breakthrough towards running large number of simulations for performances demonstration in Guided Wave Structural Health Monitoring.

REFERENCES

[1] X. Zhao, H. Gao, G. Zhang, B. Ayhan, F. Yan, C. Kwan et J. L. Rose, "Active health monitoring of an aircraft wing with embedded piezoelectric sensor/actuator network: I. Defect detection, localization and growth monitoring," *Smart materials and structures,* **16**(14), 1208, (2007).

[2] J. E. Michaels, "Detection, localization and characterization of damage in plates with an in situ array of spatially distributed ultrasonic sensors," *Smart Materials and Structures,* **17**(13), 035035, (2008).

[3] J. S. Hall et J. E. Michaels, "Minimum variance ultrasonic imaging applied to an in situ sparse guided wave array," *IEEE transactions on ultrasonics, ferroelectrics, and frequency control,* **57**,(110), 2311-2323, (2010).

[4] B. C. O. M. N. B. O. D. A. L. A Kulakovskyi, "Defect imaging on CFRP and honeycomb composite structures by guided waves generated and detected by a sparse PZT array", *Structural Health Monitoring 2017,* (2017).

[5] B. Chapuis, F. Jenson, P. Calmon, G. DiCrisci, J. Hamilton et L. Pomié, "Simulation supported POD curves for automated ultrasonic testing of pipeline girth welds", *Springer,* **58**, 433-441, (2014)

[6] C. A. Leckey, K. R. Wheeler, V. N. Hafiychuk, H. Hafiychuk et D. A. Timuçin, "Simulation of guided-wave ultrasound propagation in composite laminates: Benchmark comparisons of numerical codes and experiment," *Ultrasonics,* **84**, 187-200, (2018).

[7] Extende, "CIVA in a few words," [En ligne]. Available: http://www.extende.com/civa-in-a-few-words. [Access August 2018].

[8] G. C. Cohen and L. Qing Huo, "Higher-order numerical methods for transient wave equations.," *The Journal of the Acoustical Society of America*, 2003.

[9] F. Ben Belgacem, "The Mortar finite element method with Lagrange multipliers", *Numerische Mathematik,* **84**(12), 173-197, (1999).

[10] E. Demaldent, A. Imperiale, N. Leymarie, S. Chatillon et P. Calmon, "Smart numerical tools for fast and easy modelling of the ultrasonic testing on curved composite structures," *QNDE,* 2018.